Korean J. Chem. Eng., 32(4), 717-722 (2015)
DOI: 10.1007/s11814-014-0268-z

pISSN: 0256-1115
eISSN: 1975-7220

Enhanced separator properties by coating alumina nanoparticles with poly(2-acrylamido-2-methyl-1-propanesulfonic acid) binder for lithium-ion batteries

Kwang Man Kim*,†, Lovely Rose Hepowit, Jin-Chul Kim***, Young-Gi Lee*, and Jang Myoun Ko****

*Research Section of Power Control Devices, Electronics and Telecommunications Research Institute (ETRI), Daejon 305-700, Korea
**Department of Chemical and Biological Engineering, Hanbat National University, Daejon 305-719, Korea
***Department of Medical Biomaterials Engineering, Kangwon National University, Chuncheon, Kangwon 200-701, Korea
(*Received 12 February 2014 • accepted 11 September 2014*)

Abstract−To enhance thermal stability and high-rate capability of lithium-ion batteries, both sides of porous polyethylene (PE) and poly(vinylidene fluoride) (PVdF) separators are coated with nanosized Al_2O_3 powder and poly(2-acrylamido-2-methyl-1-propanesulfonic acid) (PAMPS) binder dispersed in acetone-water solvent. For comparison, PVdF is also used as a polymer binder for coating. The Al_2O_3/PAMPS-coated separators show an improved thermal shrinkage resistance at 120 °C and enhanced electrochemical performance of $LiCoO_2$||graphite full-cell. These improvements are due to the binding ability of PAMPS, the large surface area of the Al_2O_3 nanoparticles, and their surface hydrophilicity maintained by the PAMPS binder to exhibit outstanding wettability towards the electrolyte, resulting in the increase in discharge capacity and high-rate capability.

Keywords: Polymer Binder, Alumina Coating, Separators, Electrochemical Properties, Lithium-ion Battery

INTRODUCTION

The lithium-ion battery is one of the most common rechargeable batteries for portable electronic devices and electric vehicles due to higher energy density and no charge loss when not in use. In a lithium-ion battery, the electrochemical reaction occurs by intercalation and deintercalation of lithium ions through the separator in electrolyte medium. An ideal separator allows rapid transport of Li^+ with good mechanical stability to avoid direct contact of positive and negative electrodes to prevent electrical short-circuits. Thus, the need to improve the separator property as an important factor that affects battery performance is still increasing. In particular, the enhancement of thermal stability is necessary for a separator to avoid short-circuit problems between electrodes, occurring during odd heat generation or mechanical rupture. Another important factor to consider is the ability of separator to retain the electrolyte solution.

Most commonly used separators for conventional lithium-ion batteries are porous polyolefin membranes such as polyethylene (PE) and polypropylene, due to their advantages of good mechanical strength and electrochemical stabilities [1,2]. However, they shrivel very easily upon exposure at high temperatures. Moreover, the nonpolar PE separators have poor electrolyte retention ability to polar organic electrolytes. As a way to overcome these drawbacks, a coating process on the separator with ceramic nanoparticles has been used to enhance the membrane properties, such as the thermal stability and the wettability to non-aqueous organic electrolyte solutions [3-7]. As the ceramic nanoparticles, alumina (Al_2O_3), silica (SiO_2), zirconia (ZrO_2), titania (TiO_2), and their mixtures are now used with the poly(vinylidene fluoride) (PVdF) binder. The inclusion of ceramic particles with polymer binder has been tried to give separator coating or ceramic filler-containing separator film to play useful roles in forming particle networks (particle dispersion), inhibiting the crystallization and reorganization of polymer chains (solid plasticizer), and interacting with lithium ion species (solid solvent) [8-12]. These features eventually resulted in the enhancement of electrolyte-containing separator properties such as mechanical strength, ionic conductivity, electrochemical stability, compatibility with lithium electrode, and so on. Also, there are some commercially successful examples of ceramic separators, such as Degussa's Separion® and LG Chem's SRS® technologies.

In this work, poly(2-acrylamido-2-methyl-1-propanesulfonic acid)

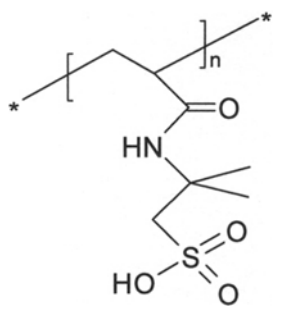

Fig. 1. Chemical structure of PAMPS.

†To whom correspondence should be addressed.
E-mail: kwang@etri.re.kr
Copyright by The Korean Institute of Chemical Engineers.

(PAMPS) as a new polymer binder of the coating matrix on PE or PVdF separator is introduced. Its chemical structure is shown in Fig. 1. The PAMPS is a water-soluble organic polymer and is often used as a protonic conductor in the solid electrolyte of electrochromic device [13], due to its controllable pH and the interfacial compatibility with conducting materials. The PAMPS also uses as an additive to ultrafiltration membrane with high water reflux [14], a solubility-increasing additive to water [15,16], and even as a proton-conductive agent in direct methanol fuel cell [17-21]. To the best of our knowledge, however, there is no report yet on the PAMPS binder applied for the separator of lithium-ion batteries. It is expected that the advantages of PAMPS as binder in the ceramic coating process will be over the role of PVdF binder. The main objective of this study was to fabricate an Al_2O_3-coated separator with PAMPS binder, which displays good thermal stability and superior wettability. In addition, a lithium-ion battery consisting of conventional $LiCoO_2$||graphite and adopting the Al_2O_3-coated separator is expected to show higher capacity and excellent high-rate capability.

EXPERIMENTAL

A fixed amount of PAMPS (Aldrich) was dissolved in water/acetone solvent mixture (5/95 v/v) and was ball-milled with Al_2O_3 powder (Degussa) overnight to yield a coating solution. Equal amounts of PAMPS and Al_2O_3 in weight basis were used. And then, both sides of PE (Celgard 2045) and PVdF (Amotech, S21216) separators were coated by dipping to the coating solution for at least 1 min to give Al_2O_3/PAMPS-coated PE and PVdF separators. The coated separators were then allowed to dry at room temperature for about 1 h and vacuum-dried at 80 °C for 24 h to remove the solvent components completely. For comparison, the Al_2O_3/PVdF-coated PE and PVdF separators were also prepared according to the same procedure above, but using PVdF binder (Aldrich) instead of PAMPS binder.

Surface morphologies of the as-prepared coated separators were observed with a field emission scanning electron microscope (Hitachi S-4800). For the coated separators, thermal stability was examined by observing the degree of thermal shrinkage after heating under vacuum at 120 °C for 1 h. The wettability was evaluated by observing the wetting trend after 1 min when a drop of electrolyte solution (1.0 M $LiPF_6$ dissolved in an equal-weight mixture of ethylene carbonate and dimethyl carbonate) (PanaX Starlyte®) was in contact with the surface of the coated separator. Pieces of the separator sample were then swollen for at least 24 h by absorbing the electrolyte solution to measure the liquid uptake. The liquid uptake (%) of coated separator was determined by a weight increase rate as $(W_2\text{-}W_1)\times100/W_1$ where W_1 and W_2 were weights of coated separators before and after absorbing the electrolyte solution for 24 h, respectively. The coated separators absorbing the electrolyte solution were also sandwiched between two Pt electrodes (1 cm× 1 cm) to measure the ionic conductivity using impedance spectroscopy function of an Autolab instrument (PGstat 100, Eco Chemie). Room-temperature ionic conductivity (σ, [Scm^{-1}]) values of the coated separators were estimated by the equation of $\sigma=l/(R\cdot A)$, where l [cm], R [Ω], and A [cm^2] denote resistance value corresponding to the radius of semicircle in the impedance spectra, thickness of the coated separator samples, and electrode area, respectively.

The coated separator was sandwiched between the cathode (Li CoO_2, Umicore KD-10) and the anode (graphite, Nihon Carbon P15B-HG) enclosed in a sealed aluminum pouch to give a lithium-ion battery full-cell. Before the final sealing of the full-cell, 35 μL of the electrolyte solution was injected to the pouch cell. All cell assemblies were conducted inside of a glove box containing an argon gas. Charging (at 0.1 C-rate) and discharging for 50 cycles were then carried out using a cycler (Toscat 3000, Toyo Systems) within the voltage range of 3.0-4.2 V, varying the C-rates as 0.1, 0.2, 0.5, 1.0, 2.0, and 5.0 to examine the high-rate capability. The 1.0 C-rate was based on the practical specific capacity of Li_xCoO_2 as 130 mAh g^{-1} (x=0.5).

RESULTS AND DISCUSSION

A mixture of acetone solvent and water non-solvent was chosen as the dissolving medium of ceramic coating solution. The pair of solvent and non-solvent may cause large difference in solubility parameters to form larger pore size and highly porous coating layers [5] through a phase-inversion technique [22-25]. In the surface morphologies (see Fig. 2), the PE and PVdF separator surfaces are adequately coated by spherical Al_2O_3 nanoparticles with pores, which are held by either PAMPS or PVdF binder. In the cases of Al_2O_3/(PAMPS and PVdF) on PE separator (see Figs. 2(c) and 2(e)), however, a deviated morphology from the spherical nanoparticles may be observed to be connected with polymer binder to yield characteristic pores. That is, the image in the Al_2O_3/PAMPS on PE separator shows prominently wrinkled morphology with larger pores but no spherical particles projected on the surface. In contrast, the sample of Al_2O_3/PVdF on PE separator (see Fig. 2(e)) exhibits homogeneously distributed spherical Al_2O_3 nanoparticles with comparatively localized larger pores. It seems to be due to the difference in binding ability between PAMPS and PVdF binders in the coating matrix. Meanwhile, the Al_2O_3/PAMPS does not homogeneously disperse on the surface of PVdF separator (see Fig. 2(d)) to show severely aggregated morphology with Al_2O_3 nanoparticles and PAMPS binder, due to an incompatibility between PAMPS and PVdF. In contrast, the Al_2O_3/PVdF on PVdF separator (see Fig. 2(f)) exhibits very smooth surface with fairly good distribution of Al_2O_3 nanoparticles. This is due to an excellent compatibility between the PVdF binder and PVdF separator.

Thermal stability is then tested by heating the Al_2O_3/PAMPS-coated separators at 120 °C for 1 h and by observing their dimensional stability (size and shape). As shown in Fig. 3, the pristine PE separator is not able to maintain its original dimension, which is shriveled enormously after exposure to the temperature environment. Meanwhile, the Al_2O_3/PAMPS-coated PE separators suffer little physical change. The PAMPS-based composite separators are almost unaffected by heating, compared to the pristine PE separator, which is severely crumpled. This means that the PE separator hardly overcomes the stress caused by the heat and is less thermally stable than the separator using PAMPS binder. The thermal stability enhanced by PAMPS can be emphasized by the chemical structure through steric hindrance of the germinal dimethyl group and the sulfomethyl group towards the amide functionality [26-29]. Thus,

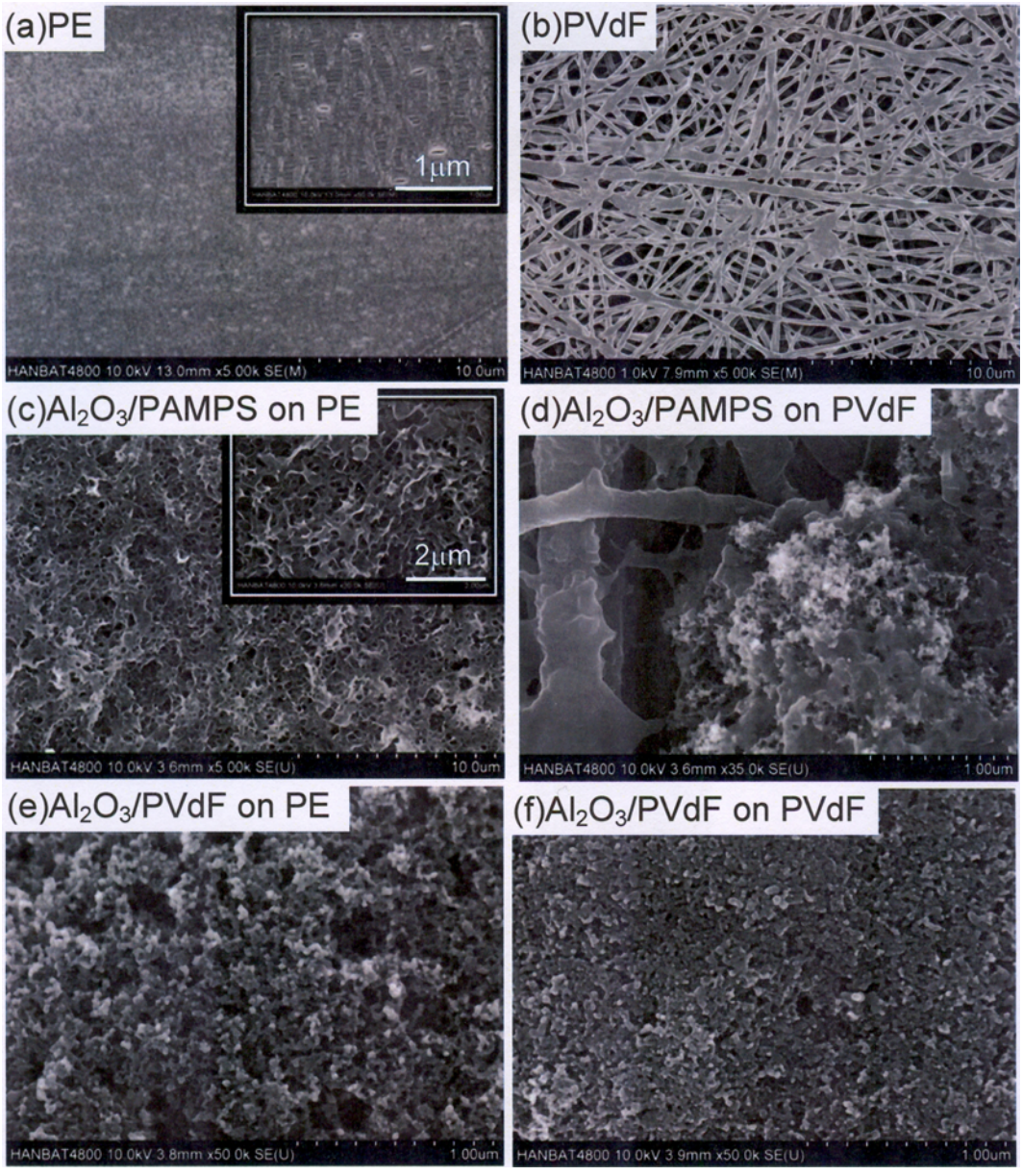

Fig. 2. Scanning electron microscopic images of (a) PE separator, (b) PVdF separator, (c) Al_2O_3/PAMPS-coated on PE, (d) Al_2O_3/PAMPS-coated on PVdF, (e) Al_2O_3/PVdF-coated on PE, and (f) Al_2O_3/PVdF-coated on PVdF.

coating the separator with Al_2O_3/PAMPS can improve the thermal stability, which is very agreed with the results reported by Choi and coworkers [3]. Meanwhile, the Al_2O_3/PAMPS-coated PVdF separator shows slightly wrinkled by the heat (see Figs. 3(c) and 3(c')), due to higher heat-resistive property of PVdF than PE. For information, the melting points of PE and PVdF are about 120-130 °C and 160-170 °C, respectively. In addition, Al_2O_3/PVdF-coated on PE and PVdF separators (not shown) are also unaffected by the heat at 120 °C, due to the heat-resistive property of PVdF.

Another important factor in the separator functions is the compatibility to liquid electrolyte solution. The wettability test is performed for the ceramic-coated separators by dropping a few microliter of the electrolyte solution and by observing the wet states after 1 min. The coated PVdF separators exhibit a comparatively better wettability towards the electrolyte solution, in contrast to the coated PE separators which are not totally wet (see Fig. 4). Also, absorption of the electrolyte solution for 24 h results in higher liquid uptake values (70-75%) for Al_2O_3-coated PVdF separators, compared to lower uptakes (30-40%) for Al_2O_3-coated PE separators. It seems that it is brought about by the large difference in polarity between nonpolar PE and highly polar PVdF separators, which is intermediated by organic electrolyte solution [4,30]. Good electrolyte retention of the PVdF-based separators may be attributed to excellent wettability of the Al_2O_3 nanoparticles towards organic electrolyte solution [5,6,31] which is further supported by the polarity of PAMPS binder [32] to be compatible with the electrolyte solution.

The ionic conductivity values are calculated using the values of electrode area (A=1 cm^2), resistance (R, see Fig. 5) and thickness

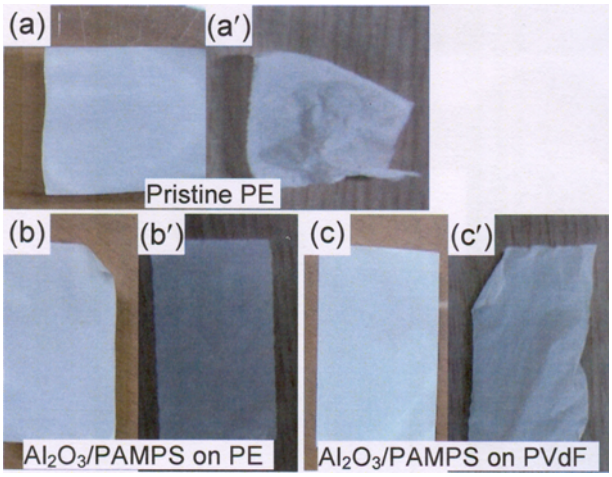

Fig. 3. Images of separators before and after the thermal shrinkage at 120 °C for 1 h: (a) pristine PE separator, (b) Al_2O_3/PAMPS-coated PE, and (c) Al_2O_3/PAMPS-coated PVdF matrices. Primed (′) images indicate the images after the thermal shrinkage.

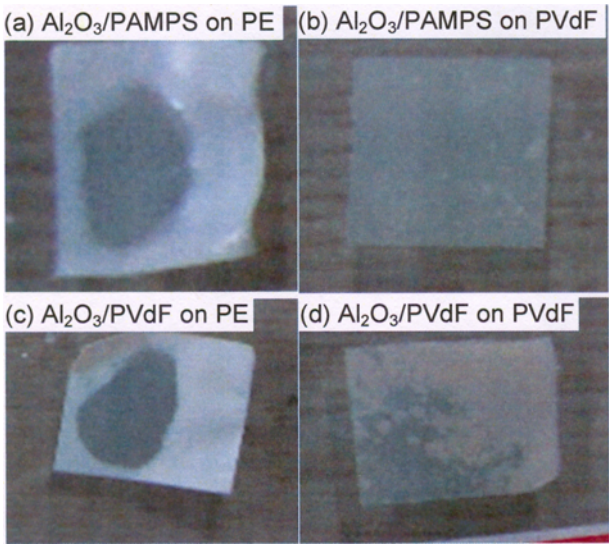

Fig. 4. Electrolyte wettability of (a) Al_2O_3/PAMPS on PE separator (b) Al_2O_3/PAMPS on PVdF separator (c) Al_2O_3/PVdF on PE separator (d) Al_2O_3/PVdF on PVdF separator.

(l) of the coated separators. Thus, room-temperature ionic conductivity values of the coated separators are determined to be 1.2×10^{-3} S cm^{-1} for Al_2O_3/PAMPS on PE (l=60 μm, R=5.04 Ω), 3.3×10^{-3} S cm^{-1} for Al_2O_3/PAMPS on PVdF (l=64 μm, R=1.97 Ω), 6.0×10^{-4} S cm^{-1} for Al_2O_3/PVdF on PE (l=68 μm, R=11.7 Ω), and 3.4×10^{-3} S cm^{-1} for Al_2O_3/PVdF on PVdF separators (l=73 μm, R=2.24 Ω). In the aspect of ionic conductivity, the coated separators with PAMPS binder exhibit higher or comparable ionic conductivity compared to the cases with PVdF binder. It may be supported by larger pores of the PAMPS-based separators, allowing faster ionic transport between the electrodes through highly porous membrane. On the other hand, the coated PVdF separators show higher ionic conductivity values than the coated PE separators. This is also due to

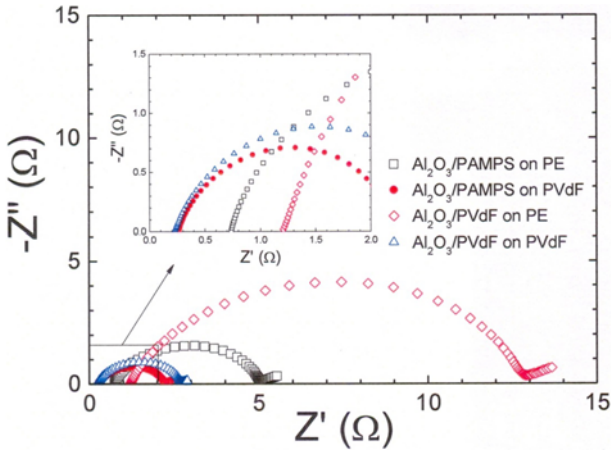

Fig. 5. Nyquist plots of Al_2O_3-coated separators for evaluation of ionic conductivity, measured between two Pt electrodes.

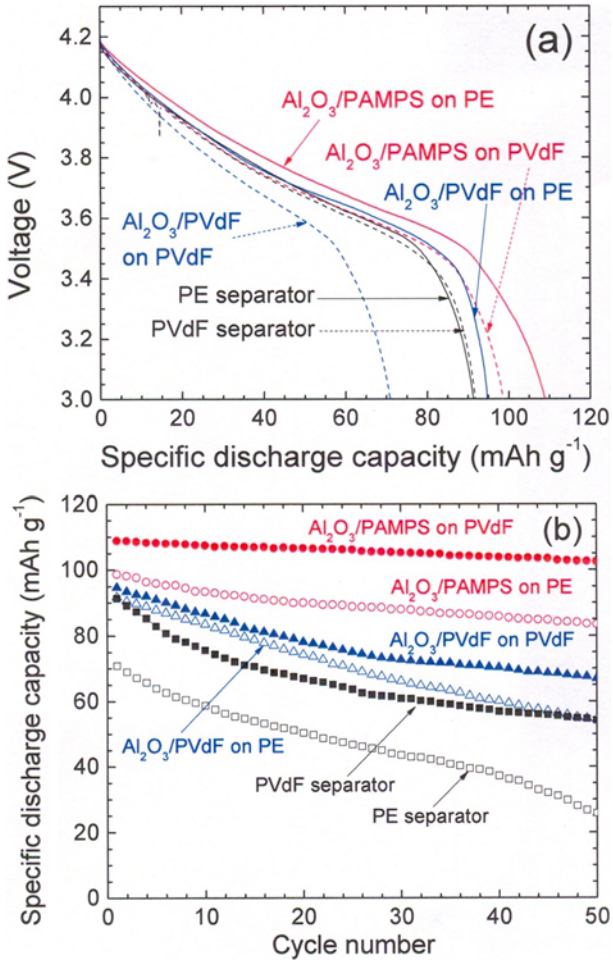

Fig. 6. (a) Initial discharge capacities and (b) cycle performance results of the $LiCoO_2$||graphite cells adopting different separator systems, obtained at 0.1 C-rate.

the larger pores of the PVdF separator itself added by the smaller pores created between interconnected inorganic Al_2O_3 nanoparticles to give better wettability towards the electrolyte solution. Com-

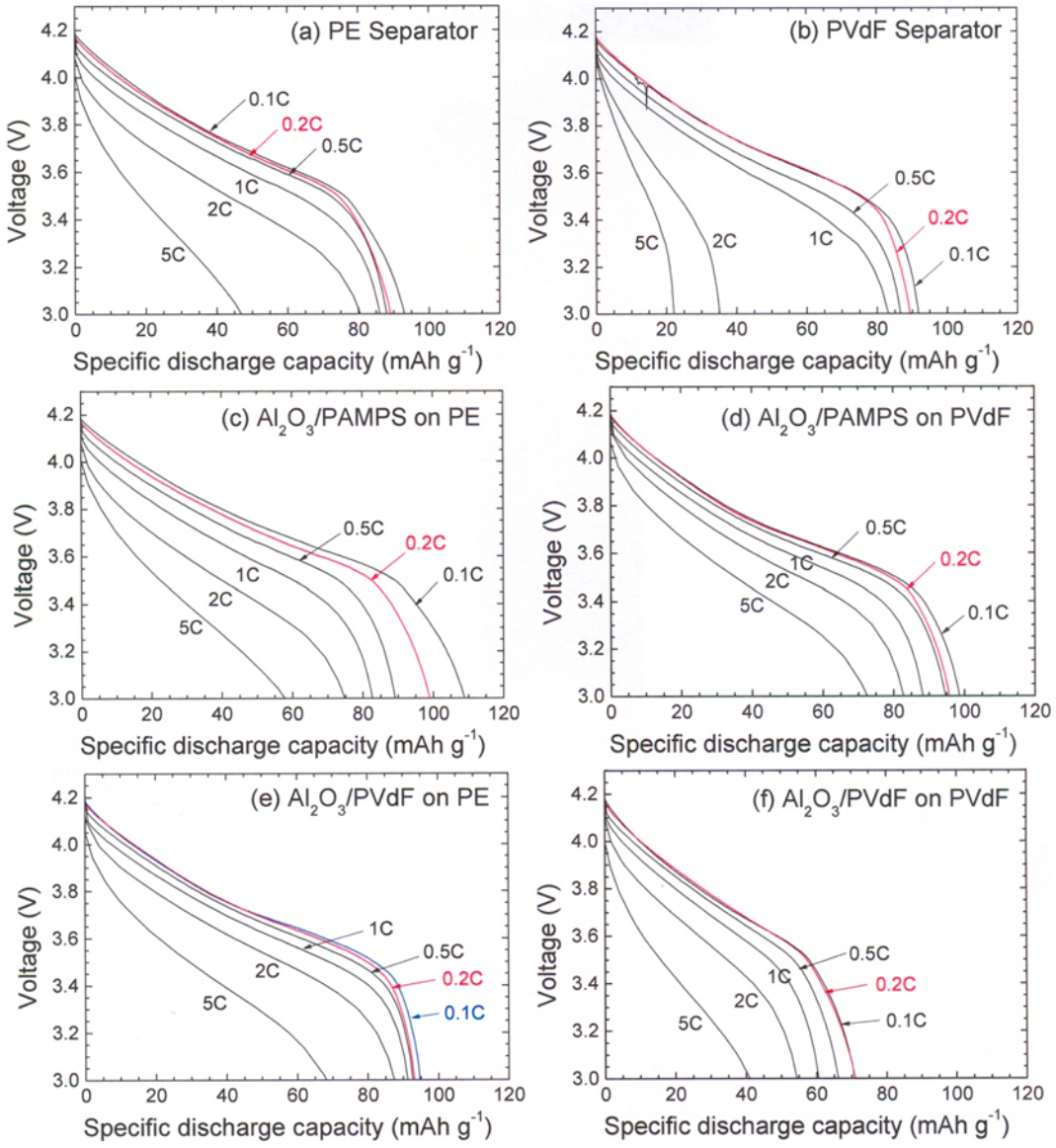

Fig. 7. Discharge capacities of the $LiCoO_2$||graphite cells containing (a) PE separator, (b) PVdF separator, (c) Al_2O_3/PAMPS on PE, (d) Al_2O_3/PAMPS on PVdF, (e) Al_2O_3/PVdF on PE, and (f) Al_2O_3/PVdF on PVdF separators.

bining all kinds of pores, the porosities may be summed up to cater facile transport of ions, and thus resulting in the enhancement of the ionic conductivity.

The effects of Al_2O_3 coatings with different polymer binders on the electrochemical performance of $LiCoO_2$||graphite full-cells adopting the coated separators are evaluated by charge-discharge test, as shown in Figs. 6 and 7. The full-cells adopting the pristine PE and PVdF separators exhibit initial discharge capacities of 91.3 and 91.8 mAh g^{-1}, respectively, at 0.1 C-rate (see Fig. 6(a)). However, the Al_2O_3-coated separators using PAMPS binder result in higher discharge capacities than those of using the pristine separators, i.e., 108 mAh g^{-1} for Al_2O_3/PAMPS on PE and 95.8 mAh g^{-1} for Al_2O_3/PAMPS on PVdF. Such increase in discharge capacity by the coating with PAMPS binder may be attributed to the large surface area of the Al_2O_3 nanoparticles with higher porosity and the binding ability of PAMPS. In contrast, the Al_2O_3/PVdF on PVdF separator shows the lowest discharge capacity (about 71 mAh g^{-1}), although it has the highest ionic conductivity value (3.4×10^{-3} S cm^{-1}). This may be due to the extremely porous structure of the Al_2O_3/PVdF on PVdF separator to be less dense and its large volume of electrolyte uptake. The extreme wettability of a separator can involve a mechanical breakdown of the separator during cycling, resulting in the lower discharge capacity. In addition, Fig. 6(b) shows cycle performance of the lithium-ion cells adopting the Al_2O_3-coated separators. It seems that the superior capacity retention ratio (94.1% for 50 cycles) for the Al_2O_3/PAMPS on PVdF may be obtained by synergistic effect between PAMPS binder (to promote closer contact between separator and electrodes, reducing interfacial and charge transfer resistances) and PVdF separator (to give higher liquid uptake and ionic conductivity).

Fig. 7 shows the rate-capability results of $LiCoO_2$||graphite full-cells adopting the coated separators. Compared to the pristine PE

separator, the Al_2O_3-coated on PE separator demonstrates large discharge capacity, e.g., at 5 C-rate, 57 mAh g^{-1} for Al_2O_3/PAMPS on PE and 68 mAh g^{-1} for Al_2O_3/PVdF on PE against 46 mAh g^{-1} for pristine PE separator. The increase in discharge capacity at high C-rates for the Al_2O_3-coated separators may be due to mainly decrease in interfacial resistance, which is followed by closer contacts between separator and electrodes, and due to slight reduction in charge transfer resistance (reflected to slight decrease in *iR* drop). Of the PVdF-based separators, the Al_2O_3/PAMPS on PVdF shows highest rate-capability, e.g., the discharge capacity of 72 mAh g^{-1} at 5 C-rate, compared to very low capacities of 35 and 22 mAh g^{-1} at 2 and 5 C-rates, respectively, for the pristine PVdF separator. Overall, the Al_2O_3-coated separator with PAMPS binder shows superior high-rate capability, due to excellent binding ability with higher heat-resistive property and higher ionic conductivity.

CONCLUSION

Al_2O_3-coated separators with PAMPS and PVdF binders were successfully prepared on pristine PE and PVdF separators to form additional smaller pores between the interconnected Al_2O_3 nanoparticles. The coated separators proved to have better thermal stability and electrolyte wettability compared to the pristine separators. The Al_2O_3/PAMPS on PE separator shows the highest initial discharge capacity (108 mAh g^{-1}) and superior high-rate capability. The improvements in the thermal stability, wettability, and electrochemical properties are attributed to thermally stable Al_2O_3 particles and the compatibility with electrolyte solution. In addition, such enhancements may be amplified by thermally stable, polar PAMPS binder for the Al_2O_3 coating. Thus, the Al_2O_3/PAMPS on PE separators can greatly contribute to use in lithium-ion batteries.

ACKNOWLEDGEMENTS

This research was supported by the Converging Research Center Program through the Korean Ministry of Science, ICT and Future Planning (2013K000218). This work was also supported by Energy Efficiency and Resources R&D Program (20112010100150) under the Korean Ministry of Trade, Industry & Energy.

REFERENCES

1. D. Linden and T. B. Reddy, *Handbook of Batteries*, 3rd Ed., McGraw-Hill (2002).
2. P. Arora and Z. Zhang, *Chem. Rev.*, **104**, 4419 (2004).
3. J.-A. Choi, S. H. Kim and D. W. Kim, *J. Power Sources*, **195**, 6192 (2010).
4. H.-S. Jeong and S.-Y. Lee, *J. Power Sources*, **196**, 6716 (2011).
5. J.-S. Jeong, S. C. Hong and S.-Y. Lee, *J. Memb. Sci.*, **364**, 177 (2010).
6. J.-H. Park, J.-H. Cho, W. Park, D. Ryoo, S.-J. Yoon, J. H. Kim, Y. U. Jeong and S.-Y. Lee, *J. Power Sources*, **195**, 8306 (2010).
7. E.-H. Kil, K.-H. Choi, H.-J. Ha, S. Xu, J. A. Rogers, M. R. Kim, Y.-G. Lee, K. M. Kim, K. Y. Cho and S.-Y. Lee, *Adv. Mater.*, **25**, 1395 (2013).
8. F. Croce, G. B. Appetecchi, L. Persi and B. Scrosati, *Nature*, **394**, 456 (1998).
9. K. M. Kim, K. S. Ryu, S.-G. Kang, S. H. Chang and I. J. Chung, *Macromol. Chem. Phys.*, **202**, 866 (2001).
10. K. M. Kim, N.-G. Park, K. S. Ryu and S. H. Chang, *Polymer*, **43**, 3951 (2002).
11. K. M. Kim, J. M. Ko, N.-G. Park, K. S. Ryu and S. H. Chang, *Solid State Ionics*, **161**, 121 (2003).
12. K. M. Kim, M. Latifatu, Y.-G. Lee, J. M. Ko, J. H. Kim and W. I. Cho, *J. Electroceram.*, **32**, 146 (2014).
13. M.-C. Bernard, A. H. Goff and W. Zeng, *Electrochim. Acta*, **44**, 781 (1998).
14. Z.-H. Zhang, Q.-F. An, T. Liu, Y. Zhou, J.-W. Qian and C.-J. Gao, *Desalination*, **297**, 59 (2012).
15. N. Hilal, L. Al-Khatib, B. P. Atkin, V. Kochkodan and N. Potapchenko, *Desalination*, **158**, 65 (2003).
16. N. Hilal, V. Kochkodan, L. Al-Khatib and T. Levadna, *Desalination*, **167**, 293 (2004).
17. J. Qiao, T. Okada and H. Ono, *Solid State Ionics*, **180**, 1318 (2009).
18. J. Qiao, T. Hamaya and T. Okada, *Chem. Mater.*, **17**, 2413 (2005).
19. J. Qiao, T. Hamaya and T. Okada, *J. Mater. Chem.*, **15**, 4414 (2005).
20. J. Qiao, T. Hamaya and T. Okada, *Polymer*, **46**, 10809 (2005).
21. J. Qiao and T. Okada, *Electrochem. Solid-State Lett.*, **9**, A379 (2006).
22. K. M. Kim, N.-G. Park, K. S. Ryu and S. H. Chang, *Electrochim. Acta*, **51**, 5636 (2006).
23. K. M. Kim, N.-G. Park, K. S. Ryu and S. H. Chang, *J. Appl. Polym. Sci.*, **102**, 140 (2006).
24. K. M. Kim, J.-C. Kim and K. S. Ryu, *Macromol. Mater. Eng.*, **291**, 1495 (2006).
25. K. M. Kim, J.-C. Kim and K. S. Ryu, *Macromol. Chem. Phys.*, **208**, 887 (2007).
26. W. O. Parker, Jr. and A. Lezzi, *Polymer*, **34**, 4913 (1993).
27. Y. A. Aggour, *Polym. Degrad. Stab.*, **44**, 71 (1994).
28. Y. A. Aggour, *Polym. Degrad. Stab.*, **60**, 317 (1998).
29. Y. A. Aggour, G. Bekhat and A. Atia, *J. Polym. Mater.*, **17**, 193 (2000).
30. J. Saunier, F. Alloin, J. Y. Sanchez and G. Caillon, *J. Power Sources*, **119-121**, 454 (2003).
31. H.-S. Jeong, D.-W. Kim, Y. U. Jeong and S.-Y. Lee, *J. Power Sources*, **195**, 6116 (2010).
32. A. M. Atta, *Polym. Adv. Technol.*, **13**, 567 (2002).